ASEAN Engineering Journal

Full Paper

BANDWIDTH AND GAIN PERFORMANCE OF REFLECTARRAY ANTENNAS FOR 5G COMMUNICATIONS: A REVIEW

Article history
Received
17 April 2024
Received in revised form
16 July 2024
Accepted
31 July 2024
Published online
28 February 2025

S. D. Khan[a], M. I. Abbasi[a*], I. M. Ibrahim[a], M. Y. Zeain[a], N. Mufti[b], M. R. Kamarudin[c], N. H. Sulaiman[d]

[a]Faculty of Electronics and Computer Technology and Engineering (FTKEK), Universiti Teknikal Malaysia Melaka (UTeM), 76100, Melaka, Malaysia.
[b]Department of Telecommunication Engineering, University of Engineering and Technology, Mardan 23200, Pakistan.
[c]Faculty of Electrical and Electronic Engineering, Universiti Tun Hussein Onn Malaysia (UTHM), Batu Pahat 86400, Johor, Malaysia.
[d]School of Electrical Engineering and Artificial Intelligence, Xiamen University Malaysia, Selangor, Malaysia.

*Corresponding author
inamabbasi@utem.edu.my

Graphical abstract

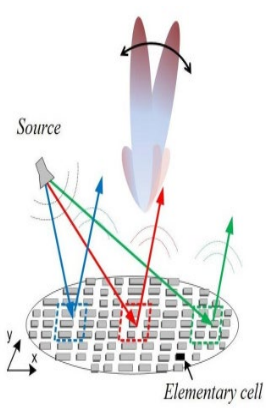

Abstract

The increasing necessity for quicker data rates in various applications is resulting in the development of future 5G/6G communication systems that possess a wider operating bandwidth. This requires the construction of appropriate antennas to meet specific parameters. Reflectarrays are being considered for 5G/6G systems because of its benefits such as because of its high gain, beam shaping, beam scanning, reconfigurability, and multi-beam capabilities. Reflectarrays are effective, although their narrowband nature has limited their use. This work comprehensively investigates the present condition of broadband reflectarrays. Wideband reflectarrays are evaluated and categorized according to four wideband phase tuning techniques. The bandwidth is analyzed and contrasted between a unit cell and reflectarray system, emphasizing the gain-bandwidth performance. Different wideband unit cell shapes are examined and categorized based on the method used for wideband phase adjustment. An analysis is conducted on how different wideband phase tuning methods affect the gain-bandwidth performance of reflectarrays. Factors taken into consideration include operating frequency, reflection phase range, substrate structure and material, aperture size, aperture efficiency (AE), focal distance, cross-polarization performance, gain, and side lobe levels. Comparisons are made between several phase tuning methods, and recommendations are given for creating reflectarrays with broad gain-bandwidth.

Keywords: Reflectarray antenna, Bandwidth, Gain, 5G,6G

1.0 INTRODUCTION

Reflectarray antennas have emerged as a promising technology for fifth generation (5G) wireless communication systems due to their high gain, low profile, low cost, and electronic beam steering capabilities. The upcoming fifth generation (5G) of wireless communications promises ultra-high data rates, low latency, and support for a massive number of connected devices to enable innovative applications. To achieve the ambitious goals of 5G, several new technologies across the protocol stack are being investigated, with advances in radio access networks being critical [1]. Reflectarray antennas have emerged as a promising technology for 5G wireless communications due to their high gain, low profile, and potential for electronic beam scanning [2],[3]. Compared to conventional parabolic reflectors or phased array systems, reflectarrays eliminate the complex feed network and enable the dynamic manipulation of radiated fields using tunable elements integrated within the unit cells [3],[4]. As we transition to higher frequencies in the mm-Wave bands for 5G, reducing loss and complexity becomes critical, and reflectarrays provide a lightweight and low-cost solution [2]. However, some intrinsic limitations around narrow bandwidth, high reflection loss, fabrication errors, scaling with frequency, and polarization still need to be addressed before widespread adoption [2],[4],[5], Reflectarrays can offer these capabilities for 5G infrastructure ranging from access points to user devices.

The elements of a reflectarray antenna are not all the same size as those of a linear array antenna. They may be thought of as a hybrid of printed array antennas and conventional parabolic reflector antennas, combining features like compact profiles and high gain from both. In addition to servicing future 5G communication networks [6],[7],[8],[9],[10],[11],[12], satellite communication systems [13],[14][15],[16],[17], and military communication activities in the Ka band [17], these antennas are specially designed for a variety of frequency ranges.

In this manuscript, authors analyze recent reflectarray designs for 5G in terms of various performance parameters and implementation considerations. This chapter analyzes and critiques recent research in reflectarray antennas for 5G applications based on the articles provided.

In this paper, critically review recent research in reflectarray antenna technologies for 5G, drawing key findings, limitations, and future research directions based on over the past decade. The analysis specifically focuses on design innovations that tackle challenges around bandwidth, gain, efficiency, beam scanning, material selection, unit cell geometry and emerging fabrication approaches. The subsequent part of this document possesses the subsequent organization. Section I provides an introduction of reflectarrays encompassing their operational principle and the development of wideband reflectarrays by chronicling the progression of various wideband techniques. Section II presents an overview of operating frequencies. Section III offers a comprehensive discussion on the gain performance of the reflectarray. Section IV offers a comprehensive discussion on the Bandwidth performance and section V Bandwidth Enhancement Techniques. The document concludes with Section VI. The overall organization of this document is demonstrated.

2.0 OPERATING FREQUENCY BANDS

The two key frequency ranges under consideration for 5G networks are the sub-6GHz and millimeter-wave (mm-Wave) bands. While the sub-6GHz band allows better propagation, coverage and the abundant spectrum in the mm-Wave band (30-300 GHz) enables the extreme data rates envisioned for 5G. From the papers surveyed, very few designs target the sub-6 GHz range [18],[19], most focus on the mm-Wave *Ka* and Q bands around 26-28GHz and 40-44GHz respectively [20],[21][22][5][23][4]. This indicates an emphasis on exploiting the available spectrum at mm-Wave bands to provide multi-gigabit speeds rather than primarily focusing on coverage. However, the higher frequencies also introduce greater path loss and atmospheric absorption, requiring the use of high gain directional antennas [24]. The dual challenges of realizing high gain reflectarrays while maintaining a wide bandwidth and beam steering capabilities need to be addressed.

3.0 GAIN PERFORMANCE OF REFLECTARRAYS

In reference [18], the concept of a closely connected dual-polarized reflectarray antenna was presented, as shown in Figure 1. This antenna comprises a dual-polarized feed antenna and a wideband dual-polarized reflecting surface. The reflective surface is made up of dual-polarized closely connected unit cells, each consisting of two types of components with perpendicular polarizations. The components include a dipole and a delay line. The reflective surface is composed of 13 x 34 components for one polarization and 26 x 11 elements for the opposite polarization. The feed antenna is a broad-spectrum dual-polarized horn antenna. Moreover, an examination of the phase error distribution on the reflecting surface is carried out. A prototype of the closely connected dual-polarized reflectarray antenna is simulated, produced, and tested to operate between 3 to 8 GHz frequencies to confirm the design's validity. The simulated findings closely match the measured results. Figure 1 shows the benefits and adverse effects for both polarizations. The simulation results indicate that the gain for X-polarization ranges from 9.4 to 19.1 dBi, whereas the AE fluctuates between 18.1% and 43.9%. The measured AE (Aperture Efficiency) fluctuates between 15.1% and 38.9%, while the measured gain ranges from 6.4 to 19.1 dBi. The simulated gain for Y-polarization exhibits a range of 11.8 to 19.0 dBi, while the simulated AE falls within a range of 14.3% to 34.1%. The measured AE ranges from 12.1% to 31.8%, while the measured gain varies from 9.3 to 17.5 dBi.

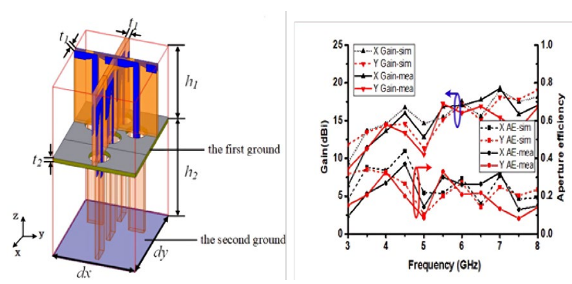

Figure 1 Tightly coupled dual polarized unit cell and Simulated [18].

Figure 2 illustrates a broadband linearly polarized single-layer reflectarray antenna described in reference [25]. This antenna is composed of spiral-dipole element cells. A method is suggested by the authors through which the phase change requirements can be fulfilled: the two degrees of freedom (TDF) elements are continuously adjusted. One can achieve a linear and seamless phase response spanning all 360 degrees by manipulating the TDF. Furthermore, the implementation of four rectangular circles encircling the spiral-dipoles facilitates a phase transition gradient that is comparatively gradual. At 6.5 and 9.5 GHz, the maximal deviations between the phase acquired by the element and the ideal phase are 20 degrees and 58 degrees, respectively; thus, the operating bandwidth is increased as shown in Figure 2. To enhance LC performance, the reflectarray element in this design is comprised of parallel H-shaped polygons on two metal layers and employs an 8 µm-thick LC layer as a varactor. The antenna's gain curve indicates a gain bandwidth of approximately 35% (6.6–9.4 GHz), or 1 dB. To attain wideband performance, the phase change is slowed via the incorporation of four rectangular rings. The antenna demonstrates a 55% AE and a gain of 26.5 dBi at 8 GHz. Based on the simulated and measured outcomes, the proposed reflectarray element is validated.

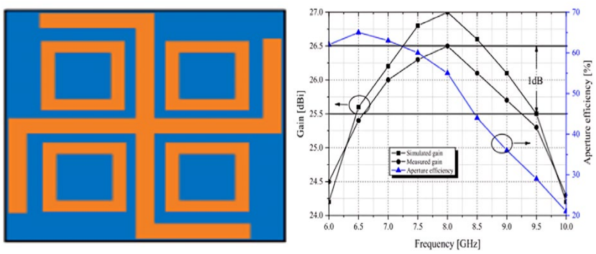

Figure 2 linearly polarized single-layer unit cell and Gain of the proposed reflectarray [25].

Furthermore, a comparison with an existing reflectarray is provided in Table I. The proposed structure overcomes bandwidth limitations caused by phase discontinuities in larger antennas. Importantly, the size of the proposed design is less than 10λ, rendering it suitable for extrapolation to higher frequencies.

Figure 3 illustrates a transmission from [26] introducing a single-layer reflectarray antenna that is linearly polarized. Phase delay lines (TGR-PDLs), which are connected to the outer ring of triple gapped rings, are used in the construction of this antenna's element cells. The new TGR-PDL element consists of three circular rings with two orthogonally positioned gaps in each ring. Furthermore, two PDLs that are the same are fastened to either half of the outer ring. First, an analysis is conducted of the attributes of the suggested element. A linear and smooth phase response spanning around 600° is obtained by varying the PDL's length. Then, using the element cell as a guide, an offset fed reflectarray antenna is developed, built, and measured with an octagon-shaped aperture of 266 mm in diameter. Verifying the proposed element's broadband property is the aim of this. According to the measurement findings, a gain bandwidth of around 31.5% at 1 dB is attained. In addition, the maximum gain at a center frequency of 10 GHz is approximately 25.78 dBi, or approximately 50% of AE. Following this, simulations are executed to determine which of several TGR-PDL geometries provides the highest bandwidth performance. The broad characteristic of the proposed element is substantiated by the constructed antenna's measured results, which confirm a 31.5% gain in bandwidth at a level of 1 dB.

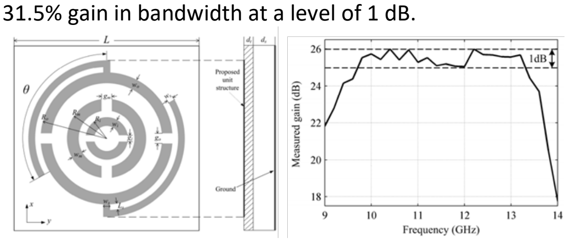

Figure 3 Proposed TGR-PDL unit cell structure, measured gain versus frequency [26].

In [21] introduces a novel circularly polarized (CP) reflectarray antenna (RRA) that is controlled by a micromotor for use in 5G communication systems' X band applications shown in Figure 4. The design incorporates concentric dual split rings capable of mechanical rotation to accomplish a phase shift of 360°. By separating the phase control mechanism and the radiation elements in an effective manner, this design minimizes element losses. At 8.3 GHz, experimental measurements of a prototype comprised of 15 15 manually rotated elements reveal an average efficiency AE of 51.8% and a maximum gain of 25.6 dB. The findings are validated by full-wave simulations, which reveal a gain bandwidth that surpasses 28.6%. An array of beam-shape experiments is conducted to further investigate the radiation capabilities of the RRA prototype. These experiments encompass square-shaped beams, cosecant-shaped beams, and large-angle scanned beams. Additional experiments with a larger-scale micromotor-controlled prototype comprising 756 elements confirm the practical applicability of the proposed design for reconfigurable high-gain antenna applications.

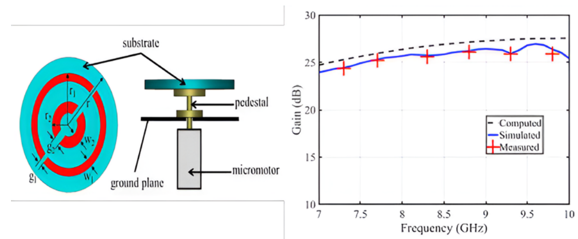

Figure 4 Proposed mechanically rotational RRA element, Computed, simulated, and measured gains versus frequency [21].

In [22], describes a design for a dual-polarized, low-profile Cassegrain reflectarray antenna operating in the W-band, featuring an integrated feed. Consider Figure 5. Ideal for in-band full-duplex (IBFD) applications, the antenna satisfies the stringent isolation criteria between its two feeding terminals. A dual-polarized planar array input is incorporated behind the primary reflectarray in the proposed antenna. The planar array feed is optimized to correspond with the reflectarray and employs methods to achieve high port isolation. Dual-layer patch cells and a rotationally symmetric layout are incorporated into the primary reflectarray in order to support dual polarization operation and large incident angles. The obtained results indicate that the impedance bandwidth spans from 93.4 to 95.6 GHz, with variations in gain not exceeding 1 dB. Across the operating spectrum, port isolation surpasses 55 dB, making it appropriate for IBFD operation. For W-band point-to-point IBFD communication systems, the design effectively illustrates a low-profile, dual-polarized Cassegrain reflectarray antenna featuring an integrated feed and exceptional isolation. A compact planar array feed in conjunction with a dual layer reflectarray that is rotationally symmetric offers a sophisticated resolution to the issues integration, profile, polarization diversity, and beam collimation. The objectives of the design are validated and the applicability for full-duplex connections is confirmed through measurements.

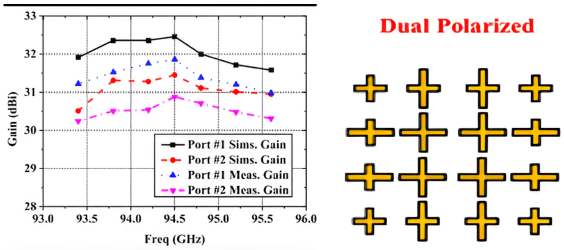

Figure 5 4 × 4 cross-slot arrays Simulated (ε_r = 2.15) and measured gain of the Cassegrain [22].

In [5], work puts forth an innovative wideband phase synthesis technique that can substantially improve the bandwidth of reflectarray antennas, irrespective of element frequency response. The key innovation lies in concurrently optimizing the reference phases at transmitting and receiving frequencies in the Ku band to minimize total phase error across the reflectarray aperture. Simulation and experimental results using simple square-ring elements demonstrate that a single-layer reflectarray with a thin substrate can achieve 16.7% measured bandwidth for under 1.5 dB gain variation, using the proposed synthesis approach. Unlike other conventional wideband reflectarray designs, the introduced phase synthesis methodology is broadly applicable to general reflectarray elements and straightforward to implement. In summary, this communication introduces a powerful new paradigm for wideband reflectarray design by decoupling phase synthesis from element frequency response characteristics shown in Figure 6. Experimental validation indicates significant bandwidth enhancement enabled by the joint optimization of transmit and receive array phases. The generality and ease of implementation of this technique could allow wideband performance to be realized using simple single-layer elements, overcoming limitations of previous reflectarray designs. This work holds great promise for adapting reflectarray antennas to modern wideband aerospace and communication applications.

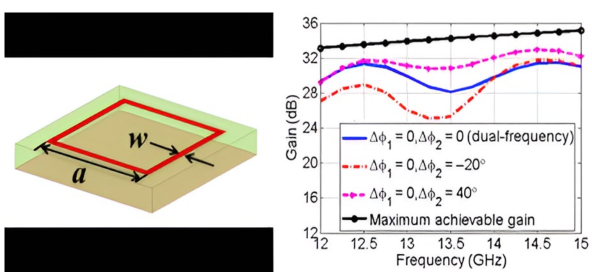

Figure 6 Geometrical configuration of a square-ring type element & Calculated gain performances using the dual-frequency approach [5].

In order to attain greater data rates and coverage areas, the gain of a reflectarray antenna is an essential input. For a greater gain to be achieved, a larger aperture size is necessary. The gain of a two-dimensional reflectarray featuring a pencil beam is greater in comparison to a linear reflectarray featuring fan beam patterns. Spillover and ohmic losses are the primary contributors to gain degradation; however, element type, position, and characteristics also exert an influence on gain. By positioning high gain, narrow beam elements in the center of the array and broad beam elements in the extremities, it is possible to attain high gain values. It is critical to regulate the level of cross-polarization and side lobes in order to attain a high gain [27],[28].

The necessity for increased gain in reflectarrays for 5G is crucial to achieve extended communication range. While most designs achieve gains ranging between 25-30 dBi, those surpassing 30 dBi are rare. Therefore, further enhancement in gain performance through optimization is needed. Various avenues, such as compact periodicity of array elements and expanded apertures, can be explored to elevate gain. The use of programmable metamaterials and megastructures also offers promising properties. Balancing gain, efficiency, and beam width through optimization can result in incremental gains of 30-40%, as shown in Table I.

4.0 BANDWIDTH OF REFLECTARRAY ANTENNA

Adequate bandwidth is crucial in 5G systems to support beam scanning and MIMO spatial multiplexing. However, many reflectarray designs in the survey have narrow bandwidths that do not meet the requirements of 5G. Some designs have achieved wider bandwidths, which are more suitable for 5G. There is potential for improvement in element designs and time delay techniques. Larger bandwidths are desired at higher mm-Wave frequencies. Wideband antenna technologies, such as fractal geometries and frequency selective surfaces, can be used to achieve larger operating ranges. Switchable components and aperture multi-layering can also contribute to wider reflections.

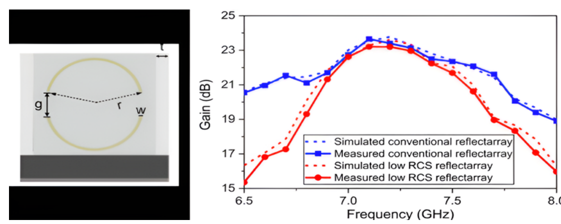

Figure 7. Unit cell structure of 3-D band stop FSS and its equivalent circuit model, simulated and measured monostatic RCS for conventional and low-RCS reflectarray [27].

In [27], Introduce an innovative approach for controlling the reflection phase response of a three-dimensional band stop structure backed by an absorbing material. By employing a cascaded arc-shaped strip resonator and absorber configuration shown in Figure 7, the authors can produce an absorption-reflection-absorption frequency response. By strategically placing metallic patches of diverse dimensions, they demonstrate the capacity to manipulate the phase of reflection within the reflection band in a flexible manner. An intriguing application of this innovative technique is in the development of a reflectarray antenna characterized by a low radar cross section and high gain. Outside the desired frequency range, the in-band phase profile of the reflecting surface is constructed optimally to collide the beam in the far field while minimizing scattering from the planar reflector. In comparison to a traditional reflectarray, the proposed low-RCS antenna maintains exceptional radiation performance, with an AE of 50.1% and a directivity of 23.5 dB. A remarkable reduction in radar cross section is achieved over a fractional bandwidth of 76.9% in the lower band and 17.1% in the upper band, with respective reduction levels of 10 dB and 8 dB. This study introduces an absorptive frequency-selective reflectarray with a controllable reflection phase response, made possible by employing three-dimensional band stop frequency selective surfaces and commercial absorbers. The design concept is successfully validated through the demonstration of a planar reflecting focusing structure with low radar cross section. The absorption-reflection-absorption frequency response is attributed to the presence of the three-dimensional band stop FSS and absorbers, while the ability to tune the reflection phase is facilitated by the inclusion of size-variable top patches. Two reflectarray antennas are fabricated and tested, one conventional and one low-RCS version as proposed in this work. The measurement results confirm that the low-RCS reflectarray exhibits comparable radiation pattern, realized gain, directivity, bandwidth, and AE to the conventional design. Additionally, significant reduction in radar cross section is achieved in the lower and upper bands. The authors provide valuable insights into the mechanism responsible for lower monostatic RCS at in-band frequencies. Overall, the simulated and measured results demonstrate excellent agreement, thereby validating the effectiveness of the proposed design methodology.

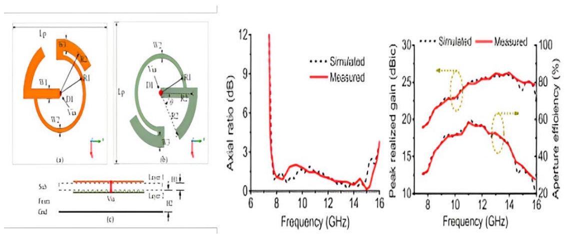

Figure 8. Configuration of the wideband unit cell, Measured and simulated AR and & peak realized gains and aperture efficiencies of the presented CP RA antenna [29].

In [29], the realm of Reflectarray Antennas (RA) catering to the demands of 5G communication, an innovative unit cell design emerges, featuring symmetrical rotational crossed dipoles to achieve a wideband Circularly Polarized (CP) antenna shown in Figure 8. The distinct characteristic of this unit cell lies in its ability to maintain a low profile while simultaneously exhibiting an impressive CP reflection bandwidth ratio of 2:1. An in-depth exploration of the proposed unit cell is undertaken, where equivalent circuit analysis and parametric studies are conducted to elucidate its operational principles. The practical manifestation of this unit cell is realized through the development of a wideband CP RA antenna, notable for its tilted beam at an angle of -20◦. Rigorous performance verification is conducted through empirical measurements. The findings indicate a 3 dB Axial Ratio (AR) bandwidth spanning 7.6–15.9 GHz, accounting for an impressive 70.6% of the total bandwidth. Additionally, the 3-dB gain bandwidth extends from 10.2–15.9 GHz, covering 43.7% of the spectrum. The antenna achieves a peak realized gain of 26.3 dBi, coupled with a maximum AE of 58.3%. Critical to the assessment of its practical utility, a meticulous comparative analysis between simulated and measured results is conducted. The congruence observed between these results underscores the reliability and efficacy of the developed CP RA antenna. This substantiates its standing as a strong contender for applications in wideband, high-gain wireless communication systems within the ambit of 5G technology.

The allocated bandwidth per operator in 5G mm-Wave bands is typically a few hundred MHz, requiring reflectarray designs to target at least 10% fractional bandwidth for practical deployments [30]. However, conventional single layer reflectarrays using resonant scattering elements suffer from narrow bandwidth due to the abrupt phase changes around resonance [31]. To address this limitation, several techniques have been proposed and demonstrated for 5G reflectarrays:

a) Use of true-time delay lines by replacing the microstrip line in each element with a meandered or stub-loaded transmission line provides a smoother phase response but increases design complexity significantly [32].
b) Employing dual or triple resonance elements such as concentric rings, spirals, or slot-loaded patches provides two degrees of controllable freedom for realizing phase requirements [5],[4],[33]. However, planar multi-resonant elements exhibit greater cross-polarization levels.
c) Implementing aperture phase synthesis or particle swarm-based optimization provides enhanced bandwidth without being restricted by element frequency response but requires extensive full-wave simulations [5],[23].
d) Polarization twisting structures and 3-D unit cells have also shown promise for bandwidth improvement [34].

Although most techniques have demonstrated over 30% bandwidth, the increased complexity can diminish practical fabrication advantages of printed reflectarrays. Ultra-wideband single-layer reflectarrays with simpler unit cells are desirable [35]. Bandwidth enhancement techniques are crucial for reflectarray design at 5G frequencies. In [36], propose novel resonant elements to achieve the necessary 360° reflection phase range for dynamic beam steering. The dual resonant elements generate 629° and 632° phase swings through proper adjustment of the bending depths, showing potential to realize reflectarrays with over 30% fractional bandwidths. However, no experimental prototypes are presented to validate the approach over an extremely wide band. In [37], experimentally demonstrate a 23% bandwidth reflectarray using single-layer rectangular patches with embedded inverted L-shaped slots. While the measured results verify stable performance from 8.6 to 10.8 GHz, higher frequencies near 30 GHz may require alternative techniques for equivalent bandwidths. The combination of multi-resonant elements and aperture stacking has shown promise for bandwidth enhancement [12].

Realizing wideband reflectarrays with low losses is also essential, especially using potentially low-cost printed circuit board (PCB) technology. The reflectarray proposed by Wu et, In [38] based on magneto-electric (ME) dipoles maintains a 34 % bandwidth for the 180°±20° reflection phase range, with an extremely low insertion loss of 0.35 dB from 10.5 to 17.8 GHz. Dynamic beams can also be generated within this entire frequency range. The planar structure is advantageous for PCB fabrication. However, the measured 11 % efficiency indicates significant room for improvement. Nonetheless, the exceptional bandwidth performance verifies the potential of ME dipole reflectarrays.

Low radar cross section (RCS) and selective frequency filtering capabilities can enhance reflectarray functionality for 5G systems. The design by Peng in [39], combines a band-notched absorber and dielectric lens to achieve an RCS reduction from 7 to 13 GHz in the horizontal polarization, with a 60 % fractional bandwidth. The pencil-beam radiation patterns at 10 GHz also demonstrate bandpass filtering with high edge selectivity and over 20 % AE from 9 to 12.6 GHz. Experimental results confirm the simulated characteristics. This exceptional RCS and frequency response control demonstrates promising device functionality. Nonetheless, further miniaturization of the unit cell thickness would aid practical device integration.

4.1 Bandwidth Enhancement Techniques

One of the main limitations of reflectarray antennas is their intrinsically narrow bandwidth due to the dependence of the reflection phase response on the frequency and incidence angle. Two key techniques have been proposed to increase bandwidth - using multi-resonant elements that provide similar reflection phases over a wide band [40],[41],[5] and shaping the reflector surface to induce spatial phase delays that compensate for frequency variations [42],[43],[44]. In [40], concentric loops are combined with attached phase delay lines to achieve 31.5%, 1-dB gain bandwidth centered at 10 GHz. The windmill structure in [41], creates a multi-resonant response using a windmill ring patch and circular ring, yielding 3-dB bandwidth over 35%. However, the measured results still show some gain variation versus frequency. An alternative approach manipulates the reflection phase curve itself [5] applies an optimization algorithm to determine the ideal reference phase at each frequency point independently. This provided 16.7% bandwidth experimentally but requires increased design complexity. Curving the reflectarray surface is another technique for bandwidth improvement by introducing controlled phase delays to compensate for frequency dependence. For example, In [42], utilizes an elliptical surface to achieve 40-50° bandwidth over 26-32 GHz, effectively increasing bandwidth 3.5 to 7.5 times. However, further work is still needed to fully characterize impacts on gain, side lobes, and cross-polarization across scan angles.

Overall, reasonable improvements in bandwidth have been achieved through intelligently combining resonant structures and manipulating phase characteristics. However, most techniques also increase design complexity significantly. Simplifying synthesis procedures while retaining wideband response remains an open challenge, especially for dual-polarized antennas. Extending operation across multiple frequency ranges also needs further work.

5.0 CONCLUSION

In this critical review paper, key innovations, and trends in reflectarray antenna technologies were discussed specifically in context of addressing challenges for 5G such as narrow bandwidth, low efficiency, and fixed radiation patterns while considering practical aspects of cost and manufacturability. Noteworthy progress has been achieved recently in bandwidth enhancement through multi-resonant geometries and elliptical shaping, improving efficiency using tunable materials and metamaterials, and enabling beam scanning either electronically through varactors or by switching between discrete reflectarrays. However, several open problems remain including simplifying synthesis procedures, quantifying impacts of emerging fabrication approaches, independently controlling dual polarization, mitigating increased loss and design complexity at mm-Wave frequencies, and comprehensively assessing tradeoffs from a system perspective. The analysis reveals multiple areas requiring further investigation - developing broadband unit cells with independent polarization control suitable for beam scanning, establishing simulation guidelines and standardized figure-of-merits to fairly evaluate contributions, and strategically applying emerging fabrication approaches to unlock unique 3D geometries. Exploring alternate biasing methodologies for tunable materials and their system impacts also offers rich possibilities for original contributions. It is hoped that the extensive literature review and insights presented here will help guide and accelerate further innovation in this promising antenna technology as communication networks transition to 5G and beyond.

Acknowledgement

This work is funded by Universiti Teknikal Malaysia Melaka (UTeM) through "UTeM Zamalah Scheme".

Conflicts of Interest

The author(s) declare(s) that there is no conflict of interest regarding the publication of this paper

References

[1] Q. Bi, 2019, "Ten Trends in the Cellular Industry and an Outlook on 6G," *IEEE Communications Magazine*, 57(12): 31–36, DOI: 10.1109/MCOM.001.1900315.

[2] M. H. Dahri, M. I. Abbasi, M. H. Jamaluddin, and M. R. Kamarudin, 2018, "A Review of High Gain and High Efficiency Reflectarrays for 5G Communications," *IEEE Access,* 6: 5973–5985, DOI: 10.1109/ACCESS.2017.2786862.

[3] S. V. Hum and J. Perruisseau-Carrier, 2014, "Reconfigurable Reflectarrays and Array Lenses for Dynamic Antenna Beam Control: A Review," *IEEE Transactions on Antennas and Propagation*, 62(1): 183–198, DOI: 10.1109/TAP.2013.2287296.

[4] J. Zhu, S. Liao, S. Li, and Q. Xue, 2022, "Additively Manufactured Metal-Only Millimeter-Wave Dual Circularly Polarized Reflectarray Antenna with Independent Control of Polarizations," *IEEE Transactions on Antennas and Propagation,* 70(10): 9918–9923, DOI: 10.1109/TAP.2022.3184474.

[5] Y. Mao, S. Xu, F. Yang, and A. Z. Elsherbeni, 2015, "A Novel Phase Synthesis Approach for Wideband Reflectarray Design," *IEEE Transactions on Antennas and Propagation,* 63(9): 4189–4193, DOI: 10.1109/TAP.2015.2447005.

[6] S. Costanzo, F. Venneri, A. Borgia, and G. Di Massa, 2020, "Dual-Band Dual-Linear Polarization Reflectarray for mmWaves/5G Applications," IEEE Access, 8: 78183–78192, DOI: 10.1109/ACCESS.2020.2989581.

[7] P. Mei, S. Zhang, and G. F. Pedersen, 2020, "A Low-Cost, High-Efficiency and Full-Metal Reflectarray Antenna with Mechanically 2-D Beam-Steerable Capabilities for 5G Applications," *IEEE Transactions on Antennas and Propagation,* 68(10): 6997–7006, DOI: 10.1109/TAP.2020.2993077.

[8] S. Costanzo, F. Venneri, A. Borgia, and G. Di Massa, 2019, "A Single-Layer Dual-Band Reflectarray Cell for 5G Communication Systems," *International Journal of Antennas and Propagation*, 2019: 8–11, DOI: 10.1155/2019/9479010.

[9] R. R. Elsharkawy, M. Hindy, A. A. Saleeb, and E. S. M. El-Rabaie, 2017, "A Reflectarray with Octagonal Unit Cells for 5G Applications," Wireless Personal Communications, 97(2): 2999–3016, DOI: 10.1007/s11277-017-4657-6.

[10] R. Elsharkawy, A. R. Sebak, M. Hindy, O. M. Haraz, A. Saleeb, and E. S. M. El-Rabaie, 2015, "Single Layer Polarization Independent

Reflectarray Antenna for Future 5G Cellular Applications," *2015 International Conference on Information and Communication Technology Research* (*ICTRC*), 9–12. DOI: 10.1109/ICTRC.2015.7156408.

[11] K. M. Mak, H. W. Lai, K. M. Luk, and C. H. Chan, 2014, "Circularly Polarized Patch Antenna for Future 5G Mobile Phones," *IEEE Access,* 2: 1521–1529, DOI: 10.1109/ACCESS.2014.2382111.

[12] M. H. Dahri, M. H. Jamaluddin, M. I. Abbasi, and M. R. Kamarudin, 2017, "A Review of Wideband Reflectarray Antennas for 5G Communication Systems," *IEEE Access*, 5: 17803–17815, DOI: 10.1109/ACCESS.2017.2747844.

[13] J. A. Encinar et al., 2018, "Dual-Polarization Reflectarray in Ku-Band Based on Two Layers of Dipole Arrays for a Transmit-Receive Satellite Antenna with South American Coverage," *International Journal of Microwave and Wireless Technologies,* 10(2): 149–159, DOI: 10.1017/S1759078717001209.

[14] R. Florencio, J. A. Encinar, R. R. Boix, V. Losada, and G. Toso, 2015, "Reflectarray Antennas for Dual Polarization and Broadband Telecom Satellite Applications," *IEEE Transactions on Antennas and Propagation*, 63(4): 1234–1246, DOI: 10.1109/TAP.2015.2391279.

[15] M. R. Chaharmir and J. Shaker, 2015, "Design of a Multilayer X-/Ka-Band Frequency-Selective Surface-Backed Reflectarray for Satellite Applications," *IEEE Transactions on Antennas and Propagation*, 63(4): 1255–1262, DOI: 10.1109/TAP.2015.2389838.

[16] S. Montori et al., 2015, "A Transportable Reflectarray Antenna for Satellite Ku-Band Emergency Communications," *IEEE Transactions on Antennas and Propagation,* 63(4): 1393–1407, DOI: 10.1109/TAP.2015.2398128.

[17] J. A. Encinar, M. Arrebola, L. F. De La Fuente, and G. Toso, 2011, "A Transmit-Receive Reflectarray Antenna for Direct Broadcast Satellite Applications," *IEEE Transactions on Antennas and Propagation,* 59(9): 3255–3264, DOI: 10.1109/TAP.2011.2161449.

[18] W. Li, H. Tu, Y. He, L. Zhang, S. W. Wong, and S. Gao, 2023, "A Novel Wideband Tightly Coupled Dual-Polarized Reflectarray Antenna," *IEEE Transactions on Antennas and Propagation,* 71(6): 5422–5427, DOI: 10.1109/TAP.2023.3262969.

[19] J. Liang and Y. Liu, 2019, "A Novel Microstrip Reflectarray Antenna with Ultra-Wideband Feed," 2019 Cross Strait Quad-Regional Radio Science and Wireless Technology Conference (CSQRWC), 1–3, DOI: 10.1109/CSQRWC.2019.8799139.

[20] K. K. Karnati, Y. Shen, M. E. Trampler, S. Ebadi, P. F. Wahid, and X. Gong, 2015, "A BST-Integrated Capacitively Loaded Patch for Ka- and X-Band Beamsteerable Reflectarray Antennas in Satellite Communications," *IEEE Transactions on Antennas and Propagation,* 63(4): 1324–1333, DOI: 10.1109/TAP.2015.2389252.

[21] X. Yang et al., 2017, "A Broadband High-Efficiency Reconfigurable Reflectarray Antenna Using Mechanically Rotational Elements," *IEEE Transactions on Antennas and Propagation,* 65(8): 3959–3966, DOI: 10.1109/TAP.2017.2708079.

[22] R. S. Hao, Y. J. Cheng, Y. F. Wu, and Y. Fan, 2021, "A W-Band Low-Profile Dual-Polarized Reflectarray with Integrated Feed for In-Band Full-Duplex Application," *IEEE Transactions on Antennas and Propagation*, 69(11): 7222–7230, DOI: 10.1109/TAP.2021.3109641.

[23] M. I. Abbasi, M. Y. Ismail, M. R. Kamarudin, and Q. H. Abbasi, 2021, "Reconfigurable Reflectarray Antenna: A Comparison between Design Using PIN Diodes and Liquid Crystals," *Wireless Communications and Mobile Computing*, 2021: 2835638, DOI: 10.1155/2021/2835638.

[24] T. S. Rappaport et al., 2013, "Millimeter Wave Mobile Communications for 5G Cellular: It Will Work!," *IEEE Access,* 1: 335–349, DOI: 10.1109/ACCESS.2013.2260813.

[25] X. Li, X. Li, Y. Y. Luo, G. M. Wei, and X. J. Yi, 2021, "A Novel Single Layer Wideband Reflectarray Design Using Two Degrees of Freedom Elements," *IEEE Transactions on Antennas and Propagation*, 69(8): 5095–5099, DOI: 10.1109/TAP.2021.3060098.

[26] C. Han, Y. Zhang, and Q. Yang, 2017, "A Broadband Reflectarray Antenna Using Triple Gapped Rings with Attached Phase-Delay Lines," *IEEE Transactions on Antennas and Propagation*, 65(5): 2713–2717, DOI: 10.1109/TAP.2017.2679493.

[27] H. Huang and Z. Shen, 2019, "Low-RCS Reflectarray with Phase Controllable Absorptive Frequency-Selective Reflector," *IEEE Transactions on Antennas and Propagation,* 67(1): 190–198, DOI: 10.1109/TAP.2018.2876708.

[28] M. R. Chaharmir, J. Shaker, N. Gagnon, and D. Lee, 2010, "Design of Broadband, Single Layer Dual-Band Large Reflectarray Using Multi Open Loop Elements," *IEEE Transactions on Antennas and Propagation,* 58(9): 2875–2883, DOI: 10.1109/TAP.2010.2052568.

[29] L. Wen, S. Gao, Q. Luo, W. Hu, B. Sanz-Izquierdo, and X. X. Yang, 2023, "Wideband Circularly Polarized Reflectarray Antenna Using Rotational Symmetrical Crossed Dipoles," *IEEE Transactions on Antennas and Propagation*, 71(5): 4576–4581, DOI: 10.1109/TAP.2023.3247943.

[30] N. E. W. U. S. E. Cases, 2021, "ALL THINGS 5G NR mmWAVE."

[31] W. Menzel, J. Li, and S. Dieter, 2009, "Folded Reflectarray Antenna Based on a Single Layer Reflector with Increased Phase Angle Range," *European Conference on Antennas and Propagation (EuCAP),* 2757–2760.

[32] E. Carrasco, J. A. Encinar, and M. Barba, 2007, "Wideband Reflectarray Antenna Using True-Time Delay Lines," IET Seminar Digest, 2007(11961).

[33] H. T. Xu, D. F. Guan, S. J. Yu, J. H. Tian, X. Y. Chen, and B. Peng, 2022, "Design of Reconfigurable Reflectarray Antenna with Wideband Beam Scanning," *2022 International Conference on Microwave and Millimeter Wave Technology (ICMMT),* 1–3, DOI: 10.1109/ICMMT55580.2022.10022612.

[34] W. An, S. Xu, F. Yang, and J. Gao, 2014, "A Ka-Band Reflectarray Antenna Integrated with Solar Cells," *IEEE Transactions on Antennas and Propagation,* 62(11): 5539–5546, DOI: 10.1109/TAP.2014.2354424.

[35] W. Han, F. Yang, J. Ouyang, and P. Yang, 2015, "Low-Cost Wideband and High-Gain Slotted Cavity Antenna Using High-Order Modes for Millimeter-Wave Application," *IEEE Transactions on Antennas and Propagation*, 63(11): 4624–4631, DOI: 10.1109/TAP.2015.2473658.

[36] M. H. Dahri, M. R. Kamarudin, M. H. Jamaluddin, M. Inam, and R. Selvaraju, 2017, "Broadband Resonant Elements for 5G Reflectarray Antenna Design," Telkomnika (Telecommunication Computing Electronics and Control), 15(2): 793–798, DOI: 10.12928/TELKOMNIKA.v15i2.6122.

[37] L. Guo, H. Yu, W. Che, and W. Yang, 2019, "A Broadband Reflectarray Antenna Using Single-Layer Rectangular Patches Embedded with Inverted L-Shaped Slots," *IEEE Transactions on Antennas and Propagation,* 67(5): 3132–3139, DOI: 10.1109/TAP.2019.2900382.

[38] W. Wu, K. D. Xu, Q. Chen, T. Tanaka, M. Kozai, and H. Minami, 2022, "A Wideband Reflectarray Based on Single-Layer Magneto-Electric Dipole Elements with 1-Bit Switching Mode," *IEEE Transactions on Antennas and Propagation,* 70(12): 12346–12351, DOI: 10.1109/TAP.2022.3209693.

[39] P. Mei, S. Zhang, Y. Cai, X. Q. Lin, and G. F. Pedersen, 2019, "A Reflectarray Antenna Designed with Gain Filtering and Low-RCS Properties," *IEEE Transactions on Antennas and Propagation*, 67(8): 5362–5371, DOI: 10.1109/TAP.2019.2911342.

[40] P. Y. Qin, Y. J. Guo, and A. R. Weily, 2016, "Broadband Reflectarray Antenna Using Subwavelength Elements Based on Double Square Meander-Line Rings," *IEEE Transactions on Antennas and Propagation,* 64(1): 378–383, DOI: 10.1109/TAP.2015.2502978.

[41] J. Zhao, C. Fu, H. Li, F. Li, and X. Hu, 2022, "A Single-Layer Broadband Ka-Band Reflectarray Using Novel Windmill Elements," *IEEE Transactions on Antennas and Propagation,* 70(11): 11167–11171, DOI: 10.1109/TAP.2022.3191442.

[42] P. Callaghan and P. R. Young, 2022, "Beam- and Band-Width Broadening of Intelligent Reflecting Surfaces Using Elliptical Phase Distribution," *IEEE Transactions on Antennas and Propagation,* 70(10): 8825–8832, DOI: 10.1109/TAP.2022.3199451.

[43] T. Smith, U. Gothelf, O. S. Kim, and O. Breinbjerg, 2014, "An FSS-Backed 20/30 GHz Circularly Polarized Reflectarray for a Shared Aperture L- and Ka-Band Satellite Communication Antenna," *IEEE Transactions on Antennas and Propagation,* 62(2): 661–668, DOI: 10.1109/TAP.2013.2292692.

[44] M. Y. Zeain, M. Abu, and S. N. Zabri, 2018, "Investigation of Printed Helical Antenna Using Varied Materials for Ultra-Wide Band Frequency," *Journal of Telecommunication, Electronic and Computer Engineering,* 10(2–7): 137–142.

[45] M. Teng, S. Yu, and N. Kou, 2023, "A Dual-Band Beam-Steering Array Antenna with Integration of Reflectarray and Phased Array," *IEEE Antennas and Wireless Propagation Letters,* 22(6): 1241–1245, DOI: 10.1109/LAWP.2023.3237633.

[46] B. Zhang, C. Jin, Q. Lv, J. Chen, and Y. Tang, 2021, "Low-RCS and Wideband Reflectarray Antenna with High Radiation Efficiency," *IEEE*

Transactions on Antennas and Propagation, 69(7): 4212–4216, DOI: 10.1109/TAP.2020.3044660.
[47] R. Deng, F. Yang, S. Xu, and M. Li, 2017, "An FSS-Backed 20/30-GHz Dual-Band Circularly Polarized Reflectarray with Suppressed Mutual Coupling and Enhanced Performance," *IEEE Transactions on Antennas and Propagation,* 65(2): 926–931, DOI: 10.1109/TAP.2016.2633159.
[48] G. Perez-Palomino et al., 2015, "Design and Demonstration of an Electronically Scanned Reflectarray Antenna at 100 GHz Using Multiresonant Cells Based on Liquid Crystals," *IEEE Transactions on Antennas and Propagation,* 63(8): 3722–3727, DOI: 10.1109/TAP.2015.2434421.
[49] R. Shamsaee Malfajani and B. Abbasi Arand, 2017, "Dual-Band Orthogonally Polarized Single-Layer Reflectarray Antenna," *IEEE Transactions on Antennas and Propagation*, 65(11): 6145–6150, DOI: 10.1109/TAP.2017.2754459.
[50] M. E. Trampler, R. E. Lovato, and X. Gong, 2020, "Dual-Resonance Continuously Beam-Scanning X-Band Reflectarray Antenna," *IEEE Transactions on Antennas and Propagation*, 68(8): 6080–6087, DOI: 10.1109/TAP.2020.2989559.
[51] Y. Cao, W. Che, W. Yang, C. Fan, and Q. Xue, 2020, "Novel Wideband Polarization Rotating Metasurface Element and Its Application for Wideband Folded Reflectarray," *IEEE Transactions on Antennas and Propagation*, 68(3): 2118–2127, DOI: 10.1109/TAP.2019.2948525.
[52] B. Liu, S. W. Wong, K. W. Tam, X. Zhang, and Y. Li, 2022, "Multifunctional Orbital Angular Momentum Generator with High-Gain Low-Profile Broadband and Programmable Characteristics," *IEEE Transactions on Antennas and Propagation*, 70(2): 1068–1076, DOI: 10.1109/TAP.2021.3111214.
[53] L. Guo, P. K. Tan, and T. H. Chio, 2016, "Single-Layered Broadband Dual-Band Reflectarray with Linear Orthogonal Polarizations," *IEEE Transactions on Antennas and Propagation*, 64(9): 4064–4068, DOI: 10.1109/TAP.2016.2574920.
[54] M. Inam, M. H. Dahri, M. H. Jamaluddin, N. Seman, M. R. Kamarudin, and N. H. Sulaiman, 2019, "Design and Characterization of Millimeter Wave Planar Reflectarray Antenna for 5G Communication Systems," *International Journal of RF and Microwave Computer-Aided Engineering*, 29(9). DOI: 10.1002/mmce.21804.
[55] X. Li et al., 2021, "Broadband Electronically Scanned Reflectarray Antenna with Liquid Crystals," *IEEE Antennas and Wireless Propagation Letters*, 20(3): 396–400, DOI: 10.1109/LAWP.2021.3051797.
[56] J. A. Encinar and J. A. Zornoza, 2004, "Three-Layer Printed Reflectarrays for Contoured Beam Space Applications," *IEEE Transactions on Antennas and Propagation*, 52(5): 1138–1148, DOI: 10.1109/TAP.2004.827506.
[57] Z. Wang et al., 2023, "W-Band Broadband Circularly Polarized Reflectarray Antenna," *Electronics*, 12(18), DOI: 10.3390/electronics12183849.
[58] R. Deng, S. Xu, F. Yang, and M. Li, 2017, "A Single-Layer High-Efficiency Wideband Reflectarray Using Hybrid Design Approach," *IEEE Antennas and Wireless Propagation Letters*, 16: 884–887, DOI: 10.1109/LAWP.2016.2613882.
[59] J. Wang, Y. Zhou, S. Gao, and Q. Luo, 2020, "An Efficiency-Improved Tightly Coupled Dipole Reflectarray Antenna Using Variant-Coupling-Capacitance Method," *IEEE Access*, 8: 37314–37320, DOI: 10.1109/ACCESS.2020.2973574.
[60] B. Mohammadi et al., 2018, "Enhanced Reflectarray Antenna Using Elements with Reduced Reflection Phase Sensitivity," *IEEE Antennas and Wireless Propagation Letters*, 17(7): 1334–1338, DOI: 10.1109/LAWP.2018.2845439.
[61] S. G. Zhou et al., 2022, "A Wideband 1-Bit Reconfigurable Reflectarray Antenna at Ku-Band," *IEEE Antennas and Wireless Propagation Letters*, 21(3): 566–570, DOI: 10.1109/LAWP.2021.3138438.
[62] L. X. Wu et al., 2022, "Wideband Dual-Feed Dual-Polarized Reflectarray Antenna Using Anisotropic Metasurface," *IEEE Antennas and Wireless Propagation Letters*, 21(1): 129–133, DOI: 10.1109/LAWP.2021.3121018.
[63] D. E. Serup, G. F. Pedersen, and S. Zhang, 2022, "Dual-Band Shared Aperture Reflectarray and Patch Antenna Array for S- and Ka-Bands," *IEEE Transactions on Antennas and Propagation*, 70(3): 2340–2345, DOI: 10.1109/TAP.2021.3111171.
[64] D. E. Serup, G. F. Pedersen, and S. Zhang, 2023, "Electromagnetically Controlled Beam-Steerable Reflectarray Antenna," *IEEE Transactions on Antennas and Propagation*, 71(5): 4570–4575, DOI: 10.1109/TAP.2023.3249627.

Appendix

Table 1 Comparison of different research work on 5G/6G reflectarray antennas

Ref.	Freq. (GHz)	Design Shape	Design Configuration	Gain (dBi)	BW (%)	Beam Scaning	Aperture Efficiency (%)
[4]	3-8	Tightly coupled element	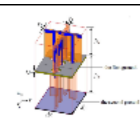	9.3-17.5	2.67:1	N/A	38.9
[25]	6.5-9.5	Spirals	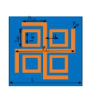	26.5	35	20°-58°	55
[26]	10	Triple Rings gaps	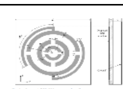	25.78	31.5	N/A	50
[21]	8.3	Crosses	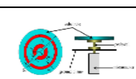	29.2	28.6	± 60°	51.8
[22]	93.4-95.6	Rings		31.86-30.88	2.3	N/A	31.4%-25.1%

Ref.	Freq. (GHz)	Design Shape	Design Configuration	Gain (dBi)	BW (%)	Beam Scaning	Aperture Efficiency (%)
[5]	12.75,13.5, 14.25	Square Rings		16.7	16.7	134°-290°	N/A
[45]	5.8,10	Circular	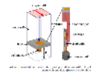	14.4-21	18	±40°	32.9-50.6
[41]	37	Windmill	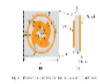	27.86	35.71	N/A	51.71
[46]	7	Cylindrical	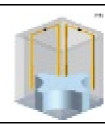	24.8	29.6	60°	60.4
[47]	20.4-30.2	Rectangular	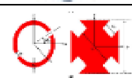	30.7-34.2	8.4/10.3	NA	64.4-65.8
[46]	6-8	pillers	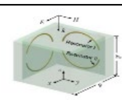	(Frictional 76.9) 17.1	66.7%,32.3% RCS reduction bands	NA	50.1
[48]	96-104	Linear unequal dipoles	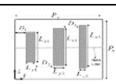	19.4	Defined by RX, TX bands	55	N/A
[49]	9.7-19.2	Circular patch	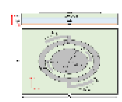	27.7-31.8	18	N/A	63-42
[50]	10.1	Cross/rings	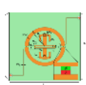	15.03	7.81	±50° continuous, dual plane	25.42
[29]	7.6–15.9	Circular Crossed Dipoles	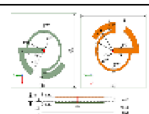	43.7	67.2	-20° tilt	58.3
[51]	29	Metasurface	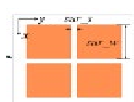	20.7	34.5	N/A	37.2
[52]	9.5–10.5	Rectangular	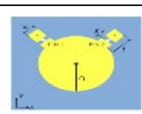	31.5	10	Reconfigurable	2.95
[53]	11.7–13.7	Rectangular	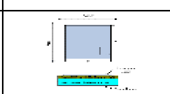	31.8-32.1	24/21	No scan	48-38
Ref.	Freq. (GHz)	Design Shape	Design Configuration	Gain (dBi)	BW (%)	Beam Scaning	Aperture Efficiency (%)
[54]	26	Rec. Patch / Cir. Patch	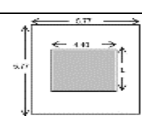	25.2-26.45	13.6-13.1	N/A	N/A

[55]	24	Circular ring		20.2	16.7	±45°	29.47
[41]	35	Windmail ring and circular ring patch	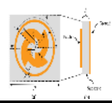	27.86	35.7	NA	51.7
[37]	10	Rectangular	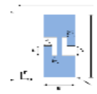	30	23	25° tilt	67
[56]	11.95	Three layers Rect, patch	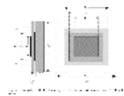	>25	10	55°	N/A
[57]	94	Rectangular	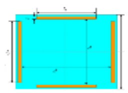	29.1	19.1	N/A	52
[58]	12-14.9	Square rings	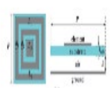	29	21.6	N/A	60,40
[59]	5	tightly coupled dipole	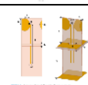	14.4-21.9	2.5:1	N/A	21.6
[40]	11	square meander-line microstrip rings	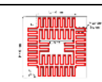	28.5-28.2	18	N/A	56.5
[60]	10	Circular rings	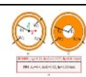	23.3	23.3	N/A	44.6
[61]	12.9–16.5	Stacked structure	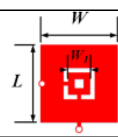	22.5	22.1	±60°	25
[62]	14.5	Blade shape	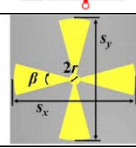	24.5	15	N/A	37.4
[63]	25.8	Stacked square patch	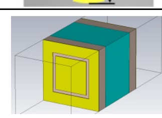	27.65	N/A	N/A	34
[64]	25	Rectangle pin actuator pins	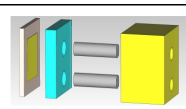	20	2GHz	120°	13.5